

Numerical Study of The Installation Configuration of Four Savonius Hydrokinetic Turbines in The Cooling Water Channel of PAITON Power Plant

Oktafika Wulaningtyas¹, Tri Yogi Yuwono^{1*}

¹Department of Mechanical Engineering, ITS, Sukolilo Surabaya 60111, Indonesia

Received: 29 October 2024, Revised: 26 February 2025, Accepted: 18 March 2025

Abstract

The energy crisis caused by decreasing fossil fuel reserves encourages the development of renewable energy, one of which is water energy from rivers, lakes, and canals. The Paiton PLTU cooling water channel, which is 2 km long, 15 m wide, and 10 m deep with a flow speed of 1-2.8 m/s, has great potential as an energy generator by installing a Savonius hydrokinetic turbine. This study aims to identify the optimal tandem spacing to avoid turbine interaction. This study uses numerical simulations using Ansys Fluent 2023 R2 with four tandem turbines rotating Counterclockwise and Clockwise. The distances between the turbines (T/D) studied are 2.1, 4.4, 60, and 300. At close T/D distances (2.1 and 4.4), the turbines influence each other, reducing the performance of the front turbine. When the distance increases to T/D = 60, the rear turbine influence decreases, so the front turbine can perform similarly to a single turbine. At T/D = 300, both turbines operate optimally with minimal interaction, achieving efficient performance and increased torque and power output.

Keywords: PAITON Power Plant, Tandem, Hydrokinetic Turbine, Savonius Turbine

1. Introduction

The energy crisis is becoming increasingly urgent due to the excessive use of fossil fuels, which not only threatens future energy supplies but also causes environmental impacts through carbon dioxide (CO_2) emissions and other greenhouse gases. In Indonesia, this issue is exacerbated by rapid population growth, reaching 281.6 million people in 2024 [1], while dependence on fossil fuels remains high and power generation capacity is still limited. To address this challenge, many countries are transitioning to renewable energy as a more sustainable primary solution.

Hydropower is a renewable energy source that can be predicted more reliably because the flow of water from rivers, lakes, and canals tends to be stable. In the cooling water canal of the Paiton Power Plant, which is 2 km long, 15 m wide, and 10 m deep, with water flowing at speeds between 1 to 2.8 m/s, this flow can be harnessed to drive turbines that convert the kinetic energy into renewable electrical energy. One example of a turbine that can be used is a hydrokinetic turbine.

Savonius water turbines are commonly used in rivers and canals due to their simple construction and low manufacturing costs [2, 3]. However, their efficiency remains a challenge, prompting extensive research to enhance their performance. To maximize energy output, multiple tur-

bines can be installed in a single water stream, but their arrangement must be optimized to prevent flow disturbances that could reduce overall efficiency. Several studies have been conducted to determine the optimal configuration for multiple turbines, ensuring better performance and energy extraction.

[4] studied the performance of Helical Savonius Hydrokinetic Turbines (HSHKT) arranged inline, using both experiments and numerical simulations. Their findings showed that increasing the distance between two turbines improved their performance, with optimum results at a 4D separation. Similarly, [5] examined the interaction between two hydrokinetic Savonius turbines arranged in line, noting that closer turbines led to stronger interaction, which weakened as the separation gap ratio (X/R) increased from 3 to 8. [6] conducted a CFD-based study on the effect of inline configuration for two drag-type hydrokinetic rotors, showing that the power coefficient of the upstream rotor increased with greater rotor distance.

[7] investigated fluid flow around four cylinders in a square configuration, analyzing the effects of Re, L/D, and fluctuating pressure. [8] studied turbulent flow around four inline square cylinders, while [9] compared 2-D and 3-D simulations of a hydrokinetic Savonius turbine array, highlighting performance differences and wake interactions. [10] examined rotor arrangement in VAWT farms, and [11] analyzed VAWT performance in urban

*Corresponding author. Email: triyogi@me.its.ac.id,
© 2025. The Authors. Published by LPPM ITS.

areas. [12] and [13] explored VAWT array interactions and power performance, while [14] proposed staggered offshore VAWT arrangements to reduce wake interference. [15] studied side-by-side VAWTs for power enhancement, and [16] addressed staggered hydrokinetic turbine arrays. [17] found optimal layouts could enhance wake energy utilization, while [18] highlighted positive interactions between Savonius-type VAWTs.

Based on the literature review, it appears that no research has yet addressed the configuration of four Savonius turbines rotating both clockwise and counterclockwise. Therefore, a study will be conducted titled Numerical study of the installation configuration of four Savonius hydrokinetic turbines in the cooling water channel of PAITON Power Plant. This research will explore the optimal arrangement and interaction effects of these turbines in the cooling water canal, which offers a promising opportunity to enhance renewable energy generation by leveraging the stable flow characteristics of the canal.

2. Numerical Simulations

2.1. Equation of Motion For The Main System Without EMVA

The study used numerical methods in ANSYS Fluent 2023 R2. The geometry of the Savonius hydrokinetic turbine was modeled in two dimensions (2D). The configuration of the Savonius hydrokinetic turbine was arranged in a tandem, with turbines rotating in both clockwise and counterclockwise directions, positioned within the cooling water channel of the Paiton Power Plant, Indonesia. The turbines were simulated in a cooling water channel

measuring 15000 mm × 10000 mm, as shown in Figure 1. The distances between the turbines (T/D) studied are 2.1, 4.4, 60, and 300.

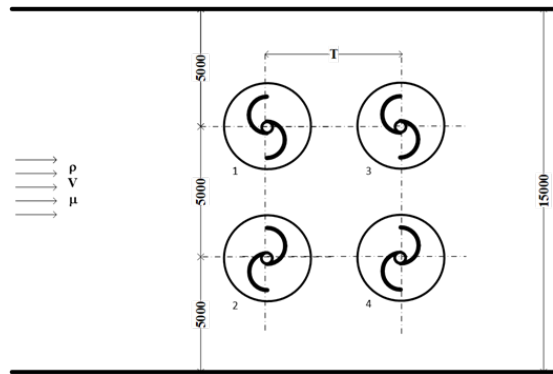


Figure 1. Schematic of the present study

2.2. Boundary Conditions and Computational Domains

The computational domain is part of a long water channel shown in Figure 2; the width of the water channel is around 13,64L, and the distance between the inlet and centre of the upstream cylinder is considered as 10L while the outlet distance from the upstream turbine is 20L. Four Savonius turbines are defined as a rotating zone along with velocity inlet, no-slip wall condition and pressure outlet, where the flow direction is from left to right. Inlet velocity is fixed at 2 m/s corresponding to the Reynolds number $3,03 \times 10^6$. The turbulence intensity set at 5% according to the study environment is ducts.

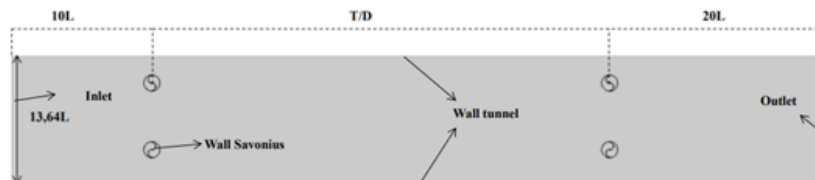


Figure 2. Computational domain

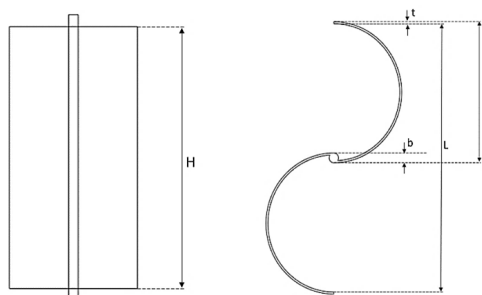


Figure 3. The geometry of the present hydrokinetic Savonius turbine

From Figure 3, Savonius hydrokinetic turbine has a blade diameter D of 578 mm and shaft rotor b of 40 mm, corresponding to the rotor diameter L of 1100 mm. This study used 3600-time steps, where the Savonius hydrokinetic turbine completed ten revolutions, with data collected from the final revolution, which was relatively stable. The quantitative data obtained includes graphs of the Coefficient of Power (CoP) and the Coefficient of Moment (Cm) as function of the Tip Speed Ratio (TSR) function, while the qualitative data consists of velocity contours. The quantitative data is calculated using the following formulas.

Tip Speed Ratio

$$\lambda = \frac{\omega \cdot R}{U} \tag{1}$$

Coefficient of Moment

$$C_m = \frac{T}{\frac{1}{2} \cdot \rho \cdot A \cdot R \cdot U^2} \tag{2}$$

Coefficient of Power

$$CoP = C_m \cdot TSR \tag{3}$$

Number of Time Steps

$$NTS = N \frac{360}{\theta} \tag{4}$$

Time Step Size

$$TSS = \frac{N}{0.15915\omega \times NTS} \tag{5}$$

2.3. Grid Independency Test and Validation

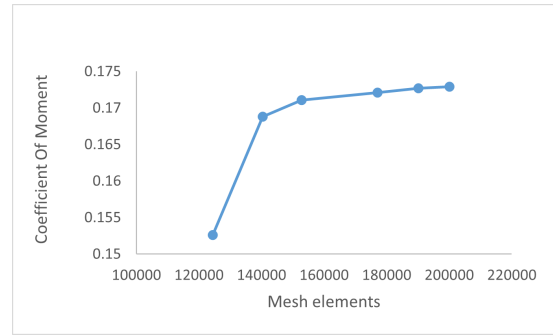


Figure 4. Grid Independence test for the present study

It is required to generate grid independency tests to determine the optimum number of elements with stable results and save the calculation cost. Six different mesh sizes were tested, ranging from 130547 to 200047 elements. The grid independent test was conducted at $TSR = 0,8$, inlet velocity = 2 m/s, and time step Δt 0.005997 s, using a 1° rotation angle. Figure 4 presents the results of the grid independency test. According to the grid-independent test, mesh 4 or 177105 is. Chosen as the present study number of meshing to save computational time and costs. The following figure contains a detailed look at the domain, rotating domain, and inflation layer of the Savonius turbine.

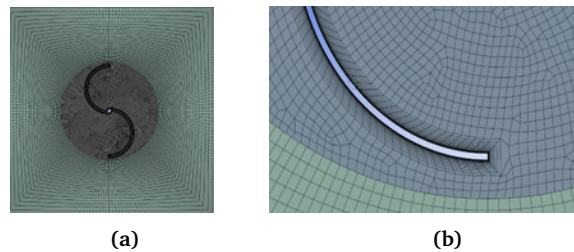


Figure 5. (a) rotating domain (b) Detail look inflation layer

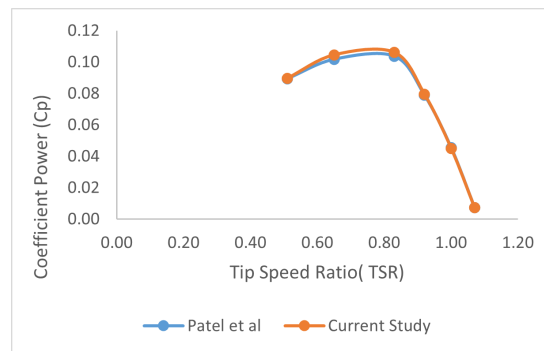


Figure 6. Comparison of the Coefficient of Power values in this study with the research of [19]

Simulation validation ensures that the model and data accurately represent the system under study. This process involves comparing current results with those from [19], specifically regarding the Coefficient of Power and TSR at a Reynolds number of 157,000. The validation indicates that the average error is below 5%, suggesting that the simulation configuration is valid. The graph in Figure 6 demonstrates consistent trends between the current study and [19]. This validation reinforces the reliability of the model in accurately representing the system.

3. Results and Discussion

In this section, the results indicate that turbine 1 and turbine 3 exhibit positive values, while turbine 2 and turbine 4 displayed negative values due to their counter-

rotating motion, the range of TSR is from 0.20 to 1.20.

3.1. Coefficient of Power

In Figure 7, the Coefficient of Power (CoP) for a single turbine and Turbines 1 and 2 follows a parabolic trend, peaking at TSR 0.6, though with lower values for Turbines 1 and 2. In contrast, Turbines 3 and 4 show a decreasing CoP as TSR increases, with significantly lower values than the single turbine and Turbines 1 and 2. At $T/D = 2.1, 4.4, \text{ and } 60$, strong wake interactions cause suboptimal performance for both turbine pairs due to turbulence and reduced water velocity. However, at $T/D = 300$, CoP values for all turbines approach those of a single turbine, indicating a more stable flow with minimal wake effects.

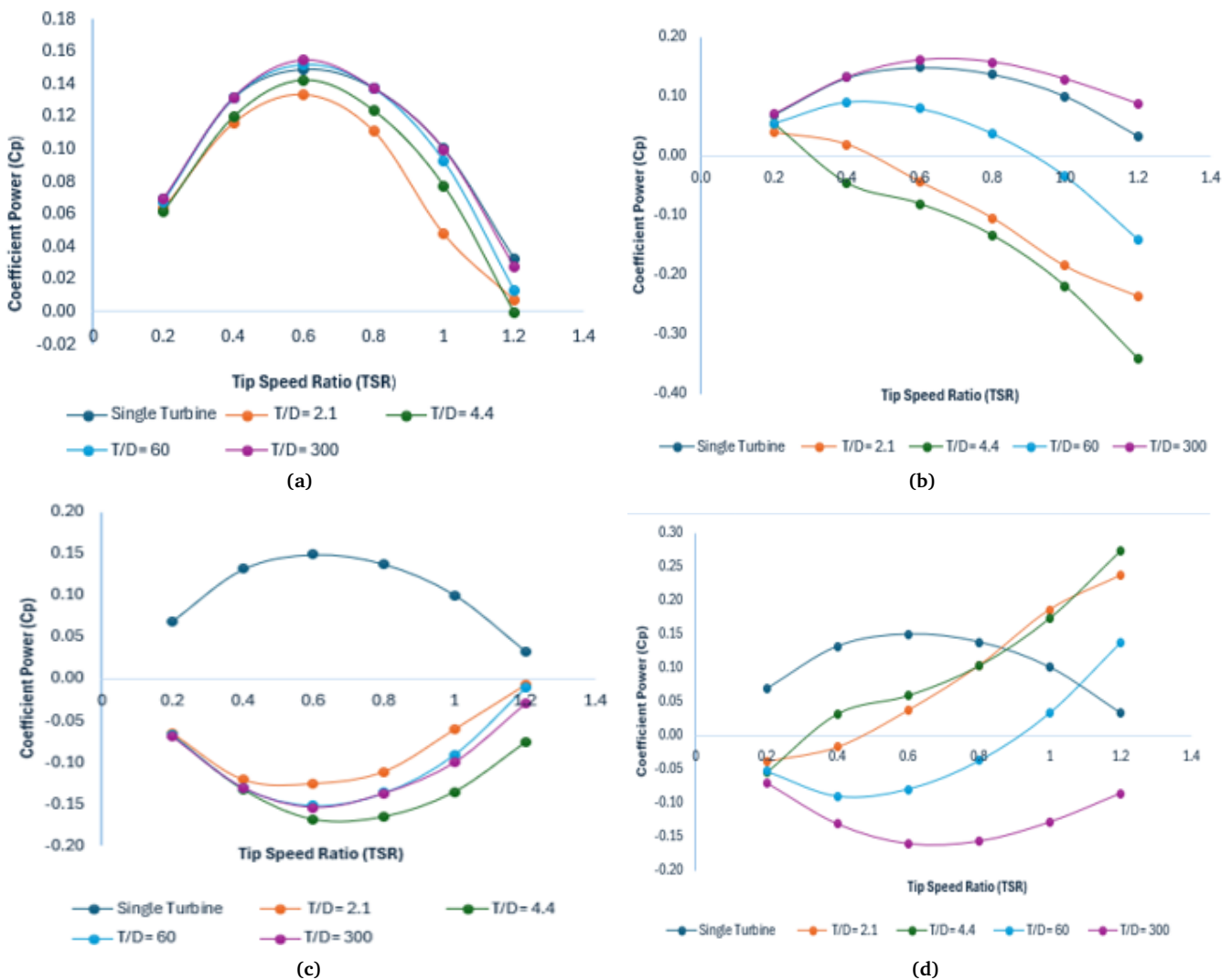


Figure 7. Evolution of Power Coefficient as function of TSR in varied relative distance (T/D) for: (a). turbine-1, (b). turbine-3, (c). turbine-2, (d). turbine-4.

3.2. Velocity Pathline at $T/D = 2.1$ and 300

In Figure 8, the water flow impacting the rear turbines (Turbines 3 and 4) has a lower velocity, shown by blue contours, compared to the higher-velocity flow on the front turbines (Turbines 1 and 2), indicated in green. At $T/D = 2.1$, this low velocity in the wake region reduces the drag force on the rear turbines, significantly lower-

ing their torque and power output. However, at $T/D = 300$, the rear turbines are no longer in the wake of the front turbines, receiving nearly equal flow velocity. As a result, their performance closely matches that of the front turbines and the single turbine, as confirmed by the Coefficient of Power (Figure 7). Furthermore, the front turbines remain unaffected by the rear turbines, further aligning their performance with the single turbine.

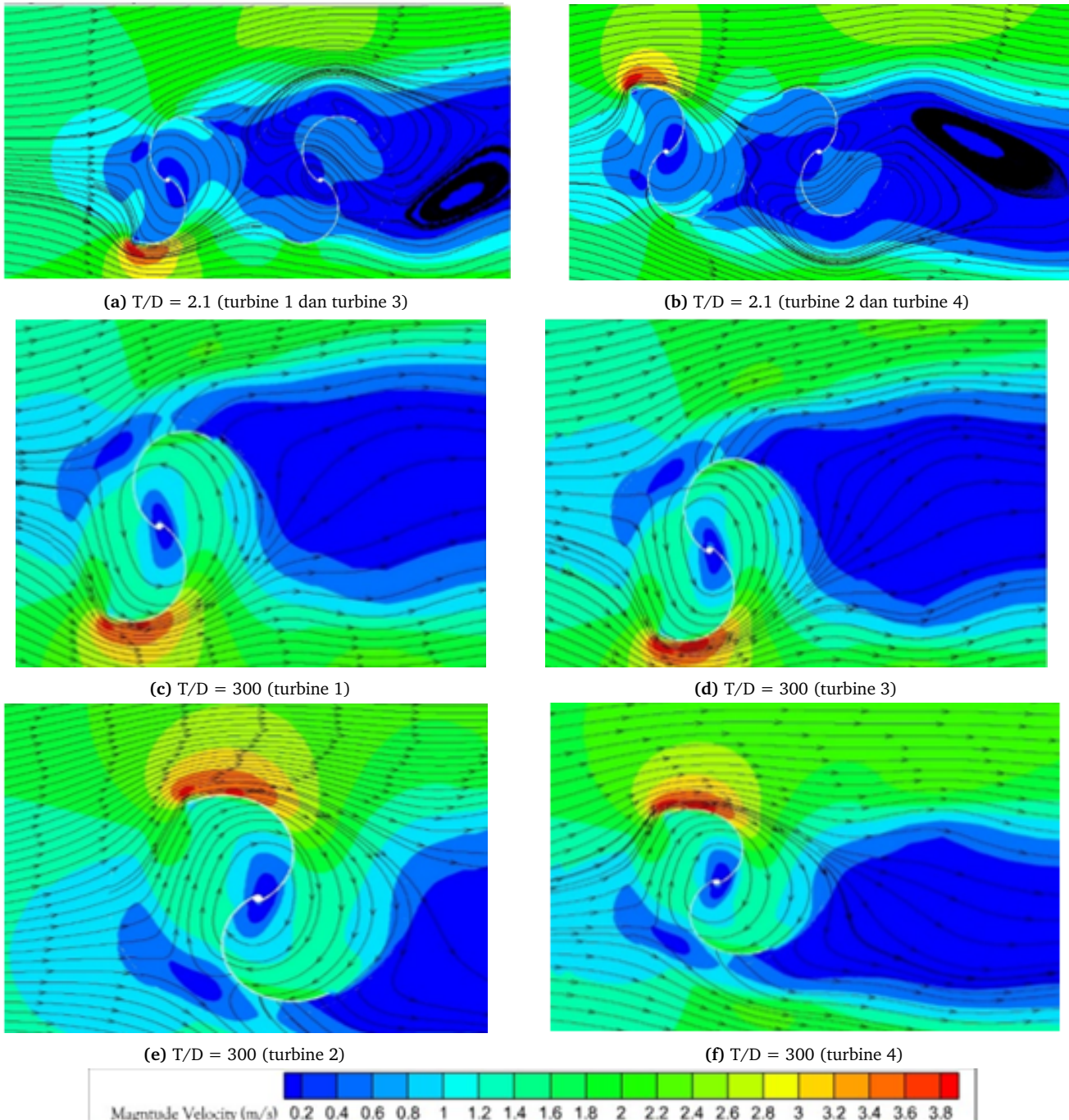


Figure 8. Comparison of the velocity pathline structure at $T/D = 2.1$ and 300, $TSR = 0.6$, $\theta = 60^\circ$

3.3. Pressure Contours at $T/D = 2.1$ and 300

Figure 9 compares the pressure contours of a single turbine and tandem turbines at a T/D distance of 2.1. The contour illustrates the pressure drop, which corresponds to the pressure difference between the front and rear sides of the turbine. For the front turbine, the presence of the

rear turbine increases the pressure behind it, reducing the pressure difference and subsequently lowering pressure drag. As a result, the torque and power output of the front turbine are lower than those of a single turbine. The rear turbine, located in the wake region, experiences low pressure, resulting in reduced drag and, thus, lower torque and power output.

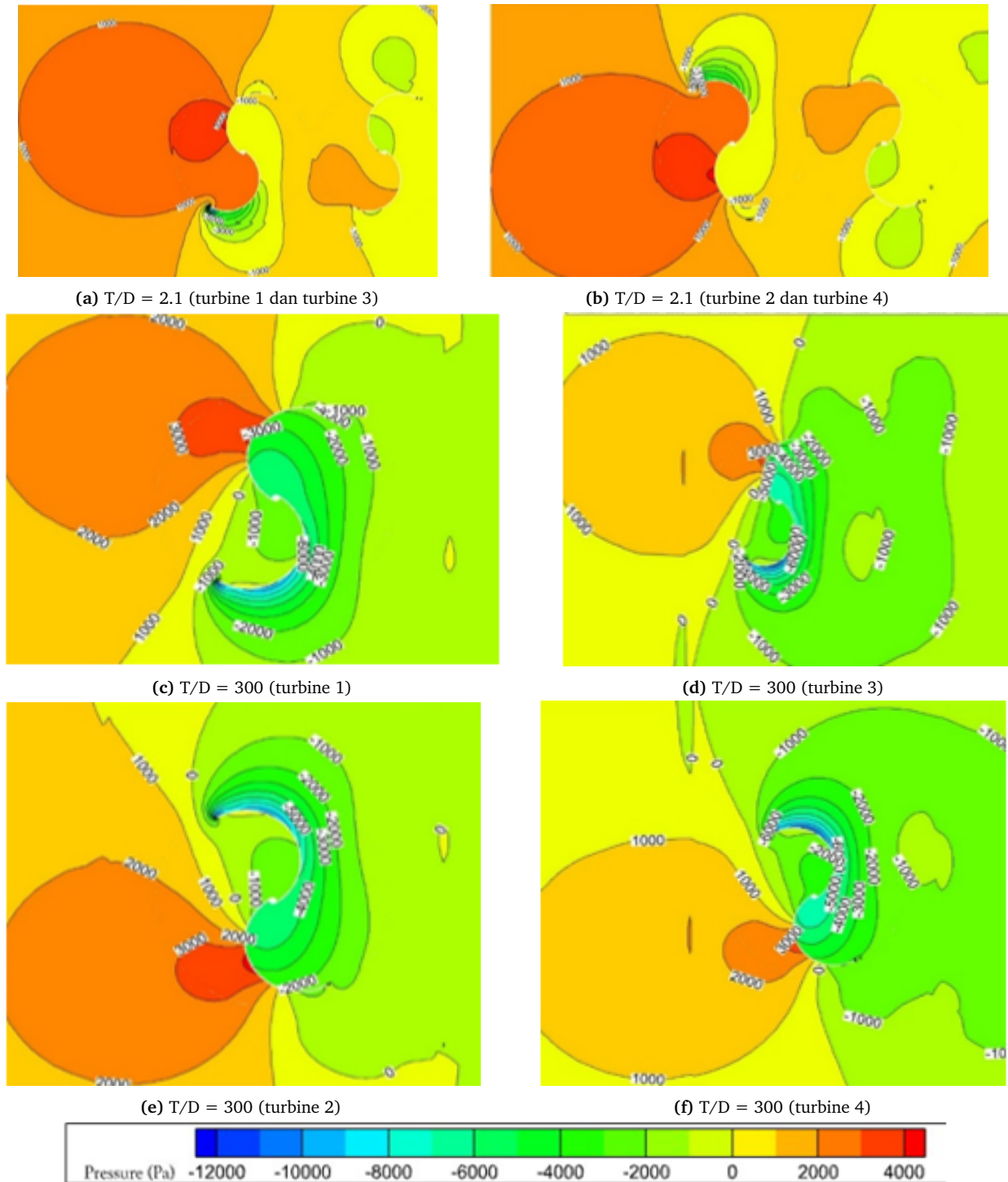


Figure 9. Comparison of the pressure contours at $T/D = 2.1$ and 300, $TSR = 0.6$, $\theta = 60^\circ$

At a T/D distance of 300, Figure 9 shows a significant pressure drop, with high pressure in front of the front turbine and low pressure behind it. The rear turbine also experiences high pressure at its front, though slightly lower than that of the front turbine, while the pressure behind it is lower than behind the front turbine. Consequently, the pressure drag on the rear turbine closely matches that of the front turbine, resulting in nearly equivalent torque and power outputs. These findings are consistent with the Coefficient of Power trends shown in Figure 7.

4. Conclusions

At close distances ($T/D = 2.1$ and 4.4), strong turbine interactions cause performance degradation in turbines 1 and 2 due to disturbances from turbines 3 and 4 behind them. Meanwhile, turbines 3 and 4, operating in the wake of turbines 1 and 2, exhibit significantly lower performance than a single turbine. As the distance increases to $T/D = 60$, the influence of turbines 3 and 4 on turbines 1 and 2 weakens, allowing turbines 1 and 2 to perform similarly to a single turbine. However, turbines 3 and 4 remain affected by wake effects, leading to reduced performance. At $T/D = 300$, turbine interactions become minimal, making it the optimal tandem configuration for both co-rotating and counter-rotating setups. With reduced wake effects, turbines 3 and 4 achieve performance levels close to turbines 1 and 2, ensuring maximum efficiency.

Acknowledgments

Our sincere appreciation goes to Prof. Dr. Ir. Tri Yogi Yuwono, DEA, IPU, AEng., for his unwavering encouragement and invaluable suggestions, which have significantly enhanced the quality and depth of this research paper on the numerical study of the installation configuration of four Savonius hydrokinetic turbines in the cooling water channel of the Paiton Power Plant.

References

- [1] B. P. Statistik, "Statistik indonesia 2024," 2024.
- [2] F. Behrouzi, M. Nakisa, A. Maimun, and Y. M. Ahmed, "Global renewable energy and its potential in malaysia: A review of hydrokinetic turbine technology," *Renewable and Sustainable Energy Reviews*, vol. 62, pp. 1270–1281, 2016.
- [3] H. J. Vermaak, K. Kusakana, and S. P. Koko, "Status of micro-hydrokinetic river technology in rural applications: A review of literature," *Renewable and Sustainable Energy Reviews*, vol. 29, pp. 625–633, 2014.
- [4] A. K. Nag and S. Sarkar, "Performance analysis of helical savonius hydrokinetic turbines arranged in array," *Ocean Engineering*, vol. 241, p. 110020, 2021.
- [5] K. Golecha, T. I. Eldho, and S. V. Prabhu, "Study on the interaction between two hydrokinetic savonius turbines," *International Journal of Rotating Machinery*, vol. 2012, no. 1, p. 581658, 2012.
- [6] Y. Zhang, C. Kang, H. Zhao, and S. Teng, "Effects of in-line configuration of drag-type hydrokinetic rotors on inter-rotor flow pattern and rotor performance," *Energy Conversion and Management*, vol. 196, pp. 44–55, 2019.
- [7] K. Lam, W. Gong, and R. So, "Numerical simulation of cross-flow around four cylinders in an in-line square configuration," *Journal of Fluids and Structures*, vol. 24, no. 1, pp. 34–57, 2008.
- [8] K. Lam and L. Zou, "Experimental study and large eddy simulation for the turbulent flow around four cylinders in an in-line square configuration," *International Journal of Heat and Fluid Flow*, vol. 30, no. 2, pp. 276–285, 2009.
- [9] Y. Chen, D. Wang, and D. Wang, "The flow field within a staggered hydrokinetic turbine array," *Renewable Energy*, vol. 224, p. 120046, 2024.
- [10] S. Sahebzadeh, A. Rezaeiha, and H. Montazeri, "Vertical-axis wind-turbine farm design: Impact of rotor setting and relative arrangement on aerodynamic performance of double rotor arrays," *Energy Reports*, vol. 8, pp. 5793–5819, 2022.
- [11] W. Xu, Y. Li, G. Li, S. Li, C. Zhang, and F. Wang, "High-resolution numerical simulation of the performance of vertical axis wind turbines in urban area: Part ii, array of vertical axis wind turbines between buildings," *Renewable Energy*, vol. 176, pp. 25–39, 2021.
- [12] M. Ahmadi-Baloutaki, R. Carriveau, and D. S.-K. Ting, "A wind tunnel study on the aerodynamic interaction of vertical axis wind turbines in array configurations," *Renewable Energy*, vol. 96, pp. 904–913, 2016.
- [13] H. Su, H. Meng, T. Qu, and L. Lei, "Wind tunnel experiment on the influence of array configuration on the power performance of vertical axis wind turbines," *Energy Conversion and Management*, vol. 241, p. 114299, 2021.
- [14] L. Kuang, H. Katsuchi, D. Zhou, Y. Chen, Z. Han, K. Zhang, J. Wang, Y. Bao, Y. Cao, and Y. Liu, "Strategy for mitigating wake interference between offshore vertical-axis wind turbines: Evaluation of vertically staggered arrangement," *Applied Energy*, vol. 351, p. 121850, 2023.
- [15] A. S. Alexander and A. Santhanakrishnan, "Mechanisms of power augmentation in two side-by-side vertical axis wind turbines," *Renewable Energy*, vol. 148, pp. 600–610, 2020.

- [16] Y. Chen, D. Zhang, P. Guo, Q. Hu, and J. Li, "A comparative analysis of 2-d and 3-d simulation for savonius hydrokinetic turbine array," *Ocean Engineering*, vol. 295, p. 116909, 2024.
- [17] B. Zhang, B. Song, Z. Mao, and W. Tian, "A novel wake energy reuse method to optimize the layout for savonius-type vertical axis wind turbines," *Energy*, vol. 121, pp. 341–355, 2017.
- [18] H. Bai and C. man Chan, "Positive interactions of two savonius-type vertical-axis wind turbines for performance improvement," *Energy Procedia*, vol. 158, pp. 625–630, 2019. Innovative Solutions for Energy Transitions.
- [19] V. Patel, G. Bhat, T. I. Eldho, and S. V. Prabhu, "Influence of overlap ratio and aspect ratio on the performance of savonius hydrokinetic turbine," *International Journal of Energy Research*, vol. 41, no. 6, pp. 829–844, 2017.